Physics Letters A 373 (2009) 1627–1631

Contents lists available at ScienceDirect

Physics Letters A

www.elsevier.com/locate/pla

Feedback controlled dephasing and population relaxation in a two-level system

Jin Wang

Department of Physics and Astronomy, The University of Tennessee at Chattanooga, Chattanooga, TN 37403-2598, USA

ARTICLE INFO

Article history:
Received 1 November 2008
Received in revised form 18 January 2009
Accepted 6 March 2009
Available online 17 March 2009
Communicated by P.R. Holland

PACS:
42.50.Lc
42.50.Ct
03.65.Bz

ABSTRACT

This Letter presents the maximum achievable stability and purity that can be obtained in a two-level system with both dephasing and population relaxation processes by using homodyne-mediated feedback control. An analytic formula giving the optimal amplitudes of the driving and feedback for the steady-state is also presented. Experimental examples are used to show the importance of controlling the dephasing process.

Published by Elsevier B.V.

1. Introduction

A central issue in quantum information processing is quantum coherence, i.e., how long a quantum state survives without decay allowing robust quantum computation [1–3]. However, real quantum systems will unavoidably be influenced by surrounding environments which gives rise to decoherence processes [4]. One type of decoherence process is called population relaxation and the other is called dephasing. Population relaxation is a dissipative decoherence process. It is described by a changing of population inversion σ_z and results in energy loss. The dephasing process is a non-dissipative process. It comes from a randomization of the phases of the atomic wave functions by thermal and vacuum fluctuations in the electromagnetic field, causing the decay of the overlap of the upper and lower state wave function [5,6]. The population of a two-level atom will not be changed during the dephasing process, but the phase of the atomic dipole will be randomized [7], or more precisely the off-diagonal density matrix elements are destroyed. As a result, the density matrix becomes a statistical mixture and thus does not display any coherence effects.

Current approaches to decoherence control can be categorized as: quantum error correction (QEC) [8–10], decoherence-free subspace (DFS) [11–15], dynamical decoupling, and quantum feedback [16,17].

The QEC approach actively corrects quantum computational errors. It accomplishes this by using proper codewords to encode the state to be protected into carefully selected subspaces of the joint Hilbert space of the system and a number of ancillary systems [8–10]. The main limitation of the QEC approach for removing decoherence is the large number of extra qubits required to store the system state. For example, correcting all possible single qubit errors requires at least five qubits [18]. The number of extra qubits increases rapidly if fault tolerant error correction is realized [13].

A DFS is a passive quantum error avoiding method, in which no measurements or recovery operations are performed to detect and correct errors [11–15]. The basic idea is to encode the information into a region of the Hilbert space where the quantum information of the system is inaccessible by the environment. Experiments successfully implementing the DFS approach have been realized in linear optics [19,20], trapped ions [21] and nuclear magnetic resonance [22,23]. The DFS approach is only possible if the system-environment interaction has certain symmetries. Unfortunately, not all quantum systems have such a region in their Hilbert space. It is theoretically known that DFS can be utilized with QEC [24], the quantum Zeno effect [25] and dynamical decoupling [26].

The dynamical decoupling scheme uses repetitive pulses to remove some of the undesirable system-environment interactions to suppress decoherence [26–33]. This technique can significantly slow down decoherence, but is not able to remove the system entropy.

The quantum feedback approach represents the earliest method for decoherence control [16,17,34]. In this approach, the quantum system of interest is subjected to continuous photodetection and the information obtained from these measurements is used to achieve control of quantum dynamics and for the preparation of desired quantum states. Manipulating quantum systems such as atoms or trapped ions by feedback is not only of fundamental theoretical interest in quantum mechanics, but also opens up possibilities to generate various interesting quantum states in the laboratory [35,36].

In this Letter we examine how well homodyne-mediated feedback can control a two-level system accounting for an additional dephasing process. We have previously investigated feedback con-

E-mail address: jin-wang@utc.edu.

0375-9601/$ – see front matter Published by Elsevier B.V.
doi:10.1016/j.physleta.2009.03.026

trol of the population relaxation process in a two-level system to achieve qubit stability [34]. However, for practical experiments it is often necessary to account for an additional non-dissipative dephasing process. The dephasing process may arise from elastic collisions in an atomic vapor, elastic phonon scattering in a solid, or photon shot noise in the measurement field [5,7,37], etc. The analysis of homodyne-mediated feedback control in which both dephasing and population relaxation processes are present thus makes our previous model more closely resemble an actual experimental realization.

Similar problems have been considered in a noisy qubit using tracking control method to maintain coherence [38]. A feedback stabilization of eigenstates of a continuously measured observable has been investigated in a higher-dimensional system [39]. The stabilization of two nonorthogonal states in a two-level system in a discreet time domain feedback scheme has also been recently studied [40].

This Letter shows that both the stability and purity of a two-level system is sensitive to the additional dephasing effect. This Letter also shows that feedback can stabilize the system state in both the upper and lower halves of the Bloch sphere in the presence of both dephasing and population relaxation. The stability of the optimal states in the upper and lower halves of the Bloch sphere are affected symmetrically by the dephasing rate. In this Letter an analytic solution for the steady-state is obtained. This leads to an analytic formula giving the optimal values of driving and feedback amplitude to maximize both stability and purity. The concluding section of this Letter discusses some experiments that may benefit from these results.

2. Feedback stabilization in the presence of dephasing and population relaxation

The system to be considered is shown in Fig. 1. The approach used in this investigation is called "Quantum Trajectories" [5,6]. We are interested in how well feedback can counter balance the effect of population relaxation with the addition of a dephasing process. We measure how well feedback works by finding the most stable pure state.

We model the dephasing process by considering the population inversion $\sigma_z = |e\rangle\langle e| - |g\rangle\langle g|$ coupled to a high temperature heat bath or vacuum fluctuations in the electromagnetic field, which can be described by an additional Hamiltonian [7]

$$H_z = \sigma_z\sqrt{\Gamma}\xi(t), \tag{1}$$

where Γ stands for the non-dissipative dephasing rate which will cause phase randomization. The term $\xi(t)$ represents Gaussian white noise [34],

By using the same method presented in Ref. [34], the homodyne-mediated feedback master equation including the non-dissipative dephasing process becomes

$$\dot{\rho} = \mathcal{L}\rho + \mathcal{K}\big(\sqrt{\gamma}\sigma\rho + \rho\sqrt{\gamma}\sigma^\dagger\big) + \frac{1}{2}\mathcal{K}^2\rho \tag{2}$$

where

$$\mathcal{L} = -i[\alpha\sigma_y, \rho] + \gamma\mathcal{D}[\sigma]\rho + \Gamma\mathcal{D}[\sigma_z]\rho. \tag{3}$$

The Liouville superoperator $\mathcal{K}$ gives reversible evolution with

$$\mathcal{K}\rho = -i[F, \rho]. \tag{4}$$

In Eqs. (2)–(4) ρ describes the system state, γ is the decay rate, $\sigma = |e\rangle\langle g|$ is the system lowering operator and the atom is driven by a resonant classical driving field with Rabi frequency 2α. The

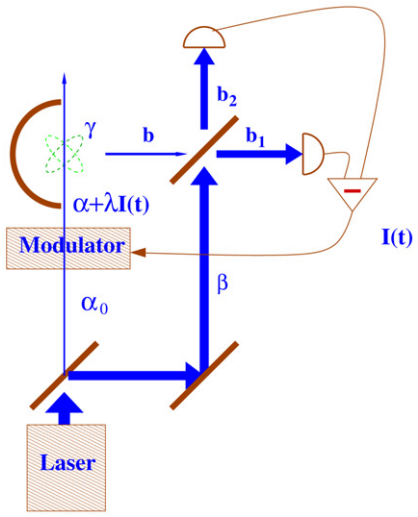

Fig. 1. Diagram of the experimental apparatus. The laser beam is split to produce both the local oscillator β and the field α_0 which is modulated using the measured homodyne photocurrent $I(t)$. The modulated beam, with amplitude proportional to $\alpha + \lambda I(t)$, drives an atom at the center of the parabolic mirror. Here λ is the feedback amplitude. The fluorescence thus collected is subject to homodyne detection using the local oscillator, and gives rise to the homodyne photocurrent $I(t)$.

Lindblad superoperator is defined as $\mathcal{D}[A]B \equiv ABA^\dagger - \{A^\dagger A, B\}/2$ [41]. The feedback Hamiltonian is given by $H_{\rm fb} = \lambda\sigma_y I(t)$, where $F = \lambda\sigma_y$ is the feedback operator and λ feedback amplitude. $I(t)$ is the photocurrent given by:

$$I(t) = \sqrt{\gamma}\langle\sigma_x\rangle_{\rm c}(t) + \xi(t). \tag{5}$$

The subscript c means conditioned.

The reason for choosing a homodyne-mediated measurement rather than a direct photodetection is because there exists an interference effect between beam b and the local oscillator β in the homodyne-mediated measurement, and it is this interference effect that leads to the deterministic part of the homodyne photocurrent proportional to $x_{\rm c} = \langle\sigma_x\rangle_{\rm c}$, where σ_x is the system x quadrature information. Obtaining system x quadrature information is essential for controlling the dynamics of the system state in the x–z plane by feedback. In the case of direct photodetection, the x quadrature information is not available.

In Eq. (2), feedback can be turned off by setting $F = 0$. In the steady-state limit, i.e., $\dot{\rho} = 0$, the following linear equations can be obtained from Eq. (2) using Bloch representation.

$$\begin{cases} (-\frac{\gamma}{4} - \sqrt{\gamma}\lambda - \Gamma - \lambda^2 - \lambda^2)x_s + (\alpha)z_s = 0, \\ (-\frac{\gamma}{4} - \Gamma)y_s + (\sqrt{\gamma} + \lambda)z_s = (-\sqrt{\gamma}), \\ (-\alpha)x + (\lambda)y_s + (-\frac{\gamma}{2} - \sqrt{\gamma}\lambda - \lambda^2)z_s = (\frac{\gamma}{2} + \sqrt{\gamma}\lambda). \end{cases} \tag{6}$$

The steady-state solution can be found analytically as follows

$$x_s = \frac{\alpha B}{D}, \qquad y_s = \frac{\alpha^2 A + C}{D}, \qquad z_s = \frac{E}{D}, \tag{7}$$

where

$$A = -\sqrt{\gamma},$$

$$B = \left(\frac{\gamma}{2} + \sqrt{\gamma}\lambda\right)\left(\frac{\gamma}{4} + \Gamma\right) - \sqrt{\gamma}\lambda,$$

$$C = \frac{\gamma}{2}\lambda\left(\frac{\gamma}{4} + \sqrt{\gamma}\lambda + \Gamma + \lambda^2\right),$$

$$E = \left(\frac{\gamma}{4} + \sqrt{\gamma}\lambda + \Gamma + \lambda^2\right)\left[\left(\frac{\gamma}{4} + \Gamma\right)\left(\frac{\gamma}{2} + \sqrt{\gamma}\lambda\right) - \sqrt{\gamma}\lambda\right],$$

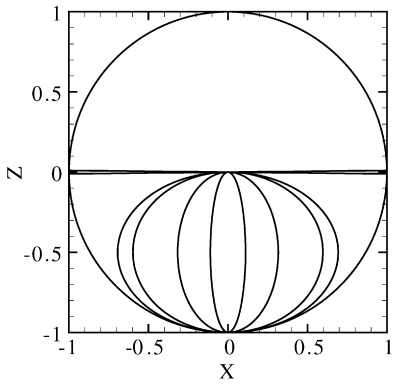

Fig. 2. The ellipses in the lower half plane represent the locus of solutions to the Bloch equations for different values of the dephasing rate Γ, optimal driving amplitude α and no feedback. From the outside ellipse in, the dephasing rate $\Gamma = 0.01, 0.1, 1, 10$ increases. The full circle (minus the points on the equator) is the locus of solutions with optimal driving and feedback for $\Gamma = 0$. The population relaxation rate is fixed at $\gamma = 1$.

$$D = -\alpha^2\left(\frac{\gamma}{4}+\Gamma\right) - \left(\frac{\gamma}{4}+\sqrt{\gamma}\lambda+\Gamma+\lambda^2\right)\left[\left(\frac{\gamma}{4}+\Gamma\right) \times \left(\frac{\gamma}{2}+\sqrt{\gamma}\lambda+\lambda^2\right) - \lambda(\sqrt{\gamma}+\lambda)\right].$$

The desired driving in terms of λ, θ, Γ, γ can be found as [42]

$$\alpha = \frac{\tan\theta[4\Gamma + (\sqrt{\gamma}+2\lambda)^2]}{4}. \tag{8}$$

This Letter measures how well decoherence is controlled by finding both the purity and stability of the system. Since

$$\mathrm{Tr}\left[\rho^2\right] = \frac{1}{2}\left(1+x^2+y^2+z^2\right) \tag{9}$$

is a measure of the purity of the Bloch sphere, $r = \sqrt{x^2+z^2}$, the distance from the center of the sphere, is also a measure of purity. Pure states correspond to $r = 1$ and maximally mixed states correspond to $r = 0$.

Eq. (8) and the steady-state solutions from Eq. (7) are used to perform the numerical simulation to search out the optimized driving and feedback amplitude by maximizing the purity r for any θ in the Bloch sphere. The numerical solution to find the parameters α and λ to maximize the purity gives the same values for α and λ as was found to maximize the stability. This is an expected result. So from this point on purity will be the only measure of how well decoherence is controlled.

When feedback is absent, the decoherence due to dephasing and population relaxation limits the locus of solutions (ellipses) to the lower half of the Bloch sphere in the x–z plane. The purity of the system as shown in Fig. 2 depends on the additional non-dissipative dephasing rate Γ. From the outside ellipse in, the dephasing rate $\Gamma = 0.01, 0.1, 1, 10$ increases. For all the plots in this Letter the population relaxation rate is fixed at $\gamma = 1$. Clearly the higher the dephasing rate, the less the purity. For each of the four dephasing rates considered, the corresponding ellipse in Fig. 2 gives the numerical results of the maximum purity for the optimized driving amplitude α.

The solutions of the Bloch equations for the dephasing rate $\Gamma = 0.01$ and population relaxation rate of $\gamma = 1$ are shown in Fig. 3. As can be seen from the figure the system purity is increased by using feedback (dashed ellipses) as compared to not using feedback (solid ellipse). In addition by using feedback the system state can be stabilized in the top half of the Bloch sphere similar to when dephasing is absent as represented by the outside circle in the figure. The figure also shows that the purity of

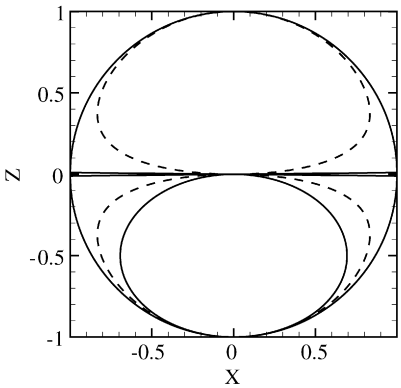

Fig. 3. The dephasing rate Γ for the ellipses inside the full circle is set to 0.01. The ellipse represented by the solid line in the lower half plane represents the solution to the Bloch equations with optimal driving and no feedback. The dashed lines represent the solutions to the Bloch equations with optimal driving and feedback. The full circle (minus the points on the equator) is the solution for the Bloch equations with optimal driving and feedback with a dephasing rate Γ of 0.

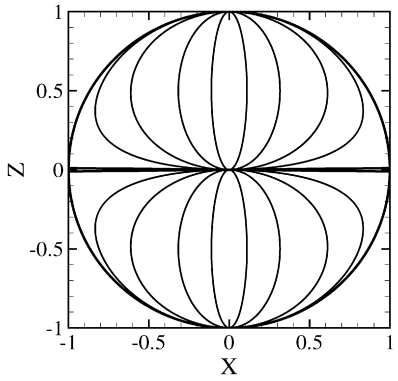

Fig. 4. The solid ellipses represent the locus of solutions to the Bloch equations with optimal feedback for multiple dephasing rates. From the outside ellipse in, we have $\Gamma = 0.01, 0.1, 1, 10$.

the optimal states in the upper half of the Bloch sphere is affected symmetrically by Γ as are those in the lower half. This contrasts to prior work [34] in which the detection efficiency is varied. As detection efficiency is decreased, the top half shrinks more quickly than the bottom half. The reason is that in the limit of the detection efficiency decreasing to zero, there is no measurement to feedback into the system and the states will be restricted to the bottom half of the Bloch sphere due to the dissipative decoherence process (from population relaxation $\gamma = 1$). When non-zero dephasing is introduced into the system the population symmetry is not changed which is expected as it is a non-dissipative process. The new physics introduced here is to illustrate that the feedback scheme provides an improvement in the purity and stability of the system as shown in Fig. 3 when non-zero dephasing is present.

Fig. 4 shows how the purity varies when using feedback for different dephasing rates Γ. The figure illustrates that purity decreases with increasing Γ. The figure also shows that optimally stabilized states still exist symmetrically in both the upper and lower halves of the Bloch sphere even with a ratio of $\Gamma/\gamma = 10$.

It is also of interest to examine the optimized driving and feedback amplitudes to achieve the maximum purity. The optimized feedback amplitude λ verses the optimized driving amplitude α for $\Gamma = 0.01$ and $\gamma = 1$ is plotted in Fig. 5. There are a few key points that can be described from the figure. First, there are two sets of optimized feedback amplitudes λ that correspond to the same driving amplitude α as defined in Eq. (8). Note that of these two sets of λ, one set corresponds to the state in the up-

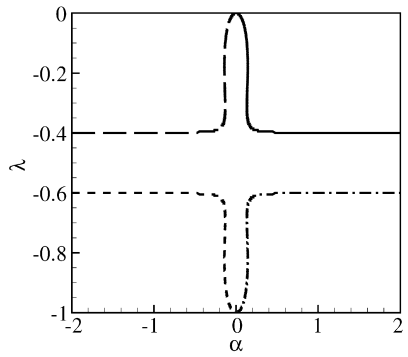

Fig. 5. The plot of optimized feedback amplitude λ verses the optimized driving amplitude α was created with $\gamma = 1$, and $\Gamma = 0.01$. Tracing each line from left to right is the same as traveling clockwise on the Bloch sphere. The solid line shows the value of optimized λ on the block sphere for $\theta = -\pi$ (the ground state) to $\theta = -\pi/2$ (the equator). The dashed line corresponds to $\theta = -\pi/2$ (the equator) to $\theta = 0$ (the excited state). The dash dotted line corresponds to $\theta = 0$ (the excited state) to $\theta = \pi/2$ (the equator). The long dashed line corresponds to $\theta = \pi/2$ (the equator) to $\theta = \pi$ (the ground state).

per half of the Bloch sphere and the other the lower half of the Bloch sphere. Second, α is antisymmetric in θ, while λ is symmetric. Third, the magnitude of the feedback is zero for $|\theta| = \pi$ (the ground state) and increases monotonically to a maximum of $\sqrt{\gamma}$ at $\theta = 0$. Fourth, the driving is zero at the ground state and at $\theta = 0$, and also changes sign as one passes through the equatorial plane. The feedback parameter λ jumps as one crosses the equatorial plane, while the driving α asymptotes to $+\infty$ on one side and $-\infty$ on the other. As shown in Fig. 3 these extreme variations in the driving do not prevent the purity from being zero in the equatorial plane. The reason for zero purity on the equatorial plane of the Bloch sphere can be understood from the solutions to the Bloch equations on the equator are not unique. This is because the master equation for $\theta_0 = \pm\pi/2$ (it is the same for both cases) has more than one null eigenvalue, and any mixture of the two equatorial states will be a stationary solution. This means that both $\rho = |\pi/2\rangle\langle\pi/2|$ and $\rho = |-\pi/2\rangle\langle-\pi/2|$ are solutions of the steady-state master equation (2). By linearity, any mixture of $|\pi/2\rangle\langle\pi/2|$ and $|-\pi/2\rangle\langle-\pi/2|$ will also be solutions. Since there is no unique solution, the system will lack stability which translates to zero purity.

3. Discussions and conclusions

The results of an experimental study from a somewhat similar system by D.I. Schuster et al. shows that dephasing is a significant factor [37]. They have found experimental dephasing time and population relaxation time for a single superconducting charge qubit strongly coupled to the cavity field of a single mode on-chip resonator. Schuster et al. found that photon shot noise in the measurement field induces qubit level fluctuations leading to dephasing. Schuster et al. also found that for weak measurement the dephasing time can be greater than 200 ns and the population relaxation time is on the order of a few microseconds. The ratio between their dephasing rate Γ and population relaxation rate γ as translated to our notation is $\Gamma/\gamma = 0.1$. Note that there is no feedback scheme used in the experiment performed by Schuster et al. This lack of feedback, according to the author's theory, causes the stability of their qubit to be confined to the lower half of the Bloch sphere. If Schuster et al. implemented our feedback scheme to counterbalance the dephasing and population relaxation effects in their system, an optimally stabilized state on the upper half of the Bloch sphere could be achieved as shown in Fig. 4.

In another paper by Bertet et al. [43], the influence of measurement induced dephasing was investigated by varying the coupling (measurement) strength between a superconducting flux qubit and a dc-SQUID based oscillator. Their experimental results showed that the dephasing time measured in a flux qubit can vary from 100 ns when the coupling is maximized to 4 μs at the optimal coupling strength. Both of these papers indicate that measurement induced dephasing is a significant factor that needs to be minimized. Of course in order for the quantum system to be used its state needs to be measured, and thus measurement induced dephasing will always be a problem. A potential method to address this problem is to use feedback to counteract the measurement induced dephasing so the system can be measured and remain in its original state. The implementation of the presented feedback scheme in the superconducting flux qubit system is an open question.

In summary, a detailed analytical and numerical analysis of using homodyne-mediated feedback scheme to control decoherence due to both dephasing and population relaxation has been provided. An analytic solution for the steady-state solution to the master equation of this system has been presented. In addition, an analytic formula to find the amount of driving and feedback amplitude to achieve optimal qubit stability and purity has been given. This Letter also shows that the stability and purity of the system in the upper and lower halves of the Bloch sphere are affected symmetrically by the additional non-dissipative dephasing effect. In conclusion, feedback can effectively counterbalance the decoherence due to both dephasing and population relaxation by stabilizing any state in the Bloch sphere except on the equator.

Acknowledgements

The author acknowledges discussions with Howard Wiseman and Gerard Milburn. The author would also like to thank The Center of Excellence in the University of Tennessee at Chattanooga for their support.

References

[1] M. Nielsen, I.L. Chuang, Quantum Computation and Quantum Information, Cambridge Univ. Press, 2000.
[2] D. Bouwmeester, A. Ekert, A. Zeilinger (Eds.), The Physics of Quantum Information, Springer, Berlin, 2000.
[3] J. Preskill, Lecture Notes on Quantum Information and Quantum Computation at http://www.theory.caltech.edu/people/preskill/ph229.
[4] W.H. Zurek, Phys. Today 44 (1991) 36.
[5] H.J. Carmichael, An Open Systems Approach to Quantum Optics, Springer-Verlag, Berlin, 1993.
[6] H.J. Carmichael, Statistical Methods in Quantum Optics, Springer-Verlag, Berlin, 1996.
[7] D.F. Walls, G.J. Milburn, Quantum Optics, Springer, Berlin, 1994.
[8] P. Shor, Phys. Rev. A 52 (1995) 2493.
[9] A.M. Steane, Phys. Rev. Lett. 77 (1996) 793.
[10] A.M. Steane, Nature 399 (1999) 124.
[11] W.H. Zurek, Phys. Today 77 (1991) 36.
[12] L.-M. Duan, G.-C. Guo, Phys. Rev. Lett. 79 (1997) 1953.
[13] P. Zanardi, M. Rasetti, Phys. Rev. Lett. 79 (1997) 3306.
[14] A. Shabani, D.A. Lidar, Phys. Rev. A 72 (2005) 042303.
[15] I.L. Chuang, D.A. Lidar, K.B. Whaley, Phys. Rev. Lett. 81 (1998) 2594.
[16] H.M. Wiseman, G.J. Milburn, Phys. Rev. Lett. 70 (1993) 548.
[17] H.M. Wiseman, Phys. Rev. A 49 (1994) 2133.
[18] J.-P. Paz, R. Laflamme, C. Miquel, W.H. Zurek, Phys. Rev. Lett. 77 (1996) 198.
[19] J.B. Altepeter, P.G. Kwiat, A.J. Berglund, A.G. White, Science 290 (2000) 498.
[20] M. Mohseni, Phys. Rev. Lett. 91 (2003) 187903.
[21] M. Bourennane, Phys. Rev. Lett. 92 (2004) 107901.
[22] D. Kielpinski, Science 291 (2001) 1013.
[23] L. Viola, Science 293 (2001) 2059.
[24] D. Bacon, D.A. Lidar, K.B. Whaley, Phys. Rev. Lett. 82 (1999) 4556.
[25] B. Tregenna, A. Beige, D. Braun, P.L. Knight, Phys. Rev. Lett. 85 (2000) 1762.
[26] L.A. Wu, D.A. Lidar, Phys. Rev. Lett. 88 (2002) 207902.
[27] L. Viola, S. Lloyd, Phys. Rev. A 58 (1998) 2733.
[28] L. Viola, E. Knill, S. Lloyd, Phys. Rev. Lett. 82 (1999) 2417.

[29] P. Zanardi, Phys. Lett. A 258 (1999) 77.
[30] D. Vitali, P. Tombesi, Phys. Rev. A 59 (1999) 4178.
[31] C. Uchiyama, M. Aihara, Phys. Rev. A 66 (2002) 032313.
[32] A.G. Kofman, G. Kurizki, Phys. Rev. Lett. 93 (2004) 130406.
[33] P. Facchi, S. Tasaki, S. Pascazio, H. Nakazato, A. Tokuse, D.A. Lidar, Phys. Rev. A 71 (2005) 022302.
[34] J. Wang, H.M. Wiseman, Phys. Rev. A 64 (2001) 063810.
[35] J.E. Reiner, W.P. Smith, L.A. Orozco, H.M. Wiseman, J. Gambetta, Phys. Rev. A 70 (2004) 023819.
[36] D.A. Steck, K. Jacobs, H. Mabuchi, T. Bhattacharya, S. Habib, Phys. Rev. Lett. 92 (2004) 223004.
[37] D.I. Schuster, A. Wallraff, A. Blais, L. Frunzio, R.-S. Huang, J. Majer, S.M. Girvin, R.J. Schoelkopf, Phys. Rev. Lett. 94 (2005) 123602.
[38] D.A. Lidar, S. Schneider, Quantum Inf. Comput. 5 (2005) 350.
[39] R. van Handel, J.K. Stockton, H. Mabuchi, IEEE Trans. Automat. Control 50 (2005) 768.
[40] A.M. Branczyk, et al., Phys. Rev. A 75 (2007) 012329.
[41] G. Lindblad, Commun. Math. Phys. 48 (1976) 199.
[42] J. Wang, H.M. Wiseman, G.J. Milburn, Special Issue of Chem. Phys. 268 (2001) 221.
[43] P. Bertet, I. Chiorescu, G. Burkard, K. Semba, C.J.P. Harmans, D.P. DiVincenzo, J.E. Mooij, Phys. Rev. Lett. 95 (2005) 257002.